Analysis and Design of a Substrate Integrated Waveguide (SIW) Cavity Slot Antenna for DSRC-Band Applications

Anil Kumar Nayak[1,2], Devraj Gangwar[1], Igor M Filanovsky[2], Kambiz Moez[2], Amalendu Patnaik[1]
Dept. of Electronics and Communication Engineering[1], Dept. of Electrical and Computer Engineering [2]
Indian Institute of Technology Roorkee[1], University of Alberta[2]
Roorkee-247667, Uttarakhand, India.[1], Edmonton, Alberta, Canada[2]
Email: anayak@ec.iitr.ac.in

***Abstract*—This paper presents a substrate integrated waveguide (SIW) cavity slot antenna for the dedicated short-range communication (DSRC) band. The DSRC band (5.9 GHz) covers the vehicle-to-vehicle communication frequency range. Conductor-backed coplanar waveguide is used to feed the antenna. To ensure the improvement in the bandwidth, the out-of-band harmonics are suppressed by employing two quarter wave resonators and a shorting pin in the feed of the antenna. The antenna radiation characteristics are also improved by good impedance matching that is achieved by placing two between the radiating patches. The SIW concept implemented in the antenna is reducing the cross-polarization level and lateral leakage. The antenna is designed, fabricated, and measured to validate the design approach. The antenna achieves fractional bandwidth of 8.8%, with the gain of 7.45 dBi. Furthermore, the measurement also indicated the radiation efficiency of 88.68% and cross-polarization level below -33 dB.**

***Index Terms*—DSRC, impedance matching, substrate integrated waveguide (SIW), radiation efficiency, vehicle-to-vehicle communication.**

I. Introduction

The vehicle wireless communication protocol began with low overhead operations under IEEE 802.11a standards, as reported in [1]. However, as time passed, the IEEE working group amended the IEEE 802.11a standards to include wireless access in vehicular environments (WAVE), which has formed the foundation of dedicated short-range communication (DSRC) in supporting intelligent transportation systems (ITS) applications. The WAVE facilitates communication between vehicle to vehicle (V2V) and vehicle to roadside information (V2I) within the 5.9 GHz frequency band (5.85 - 5.925 GHz) [2]. The vehicle-to-everything (V2X) communication is used to collect, analyze, and share information from various infrastructures [3]. Antennas having an omnidirectional radiation pattern and high gain are greatly desired in these kinds of communication systems to effectively gather environmental data. It also requires low profile, low loss, and low cross-polarization level for V2X, as reported in [4], [5].

Substrate Integrated Waveguide (SIW) technology is essential in developing planar antenna due to its ability to handle high power with a high-quality factor at higher frequencies and integrate active elements, passive elements, and antennas on the same substrate [6]–[8].

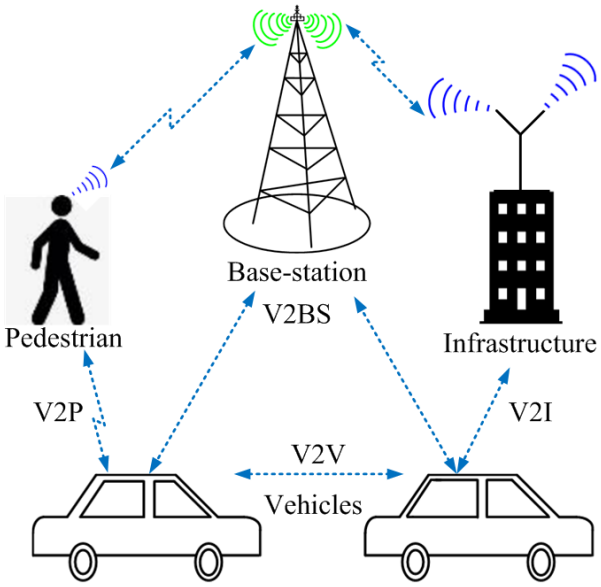

Fig. 1. Application scenarios of proposed antenna.

In this work, an effort has been made to design a SIW cavity slot antenna for DSRC band application. This is done using two quarter-wavelength resonators along with a shorting pin in the feed line. The shorting pin plays a significant role in tuning the input impedance for matching between the feed line and the patch. The gap between the feed line and patch generates the electric coupling, which helps to achieve the desired resonant frequency and improve the impedance bandwidth. Two L-shaped stubs are placed between two radiating patches, which results in an enhancement of radiation characteristics. The use of SIW-based planar antennas is justified here due to the reason that it helps to achieve less cross-polarization levels than in their other realizations

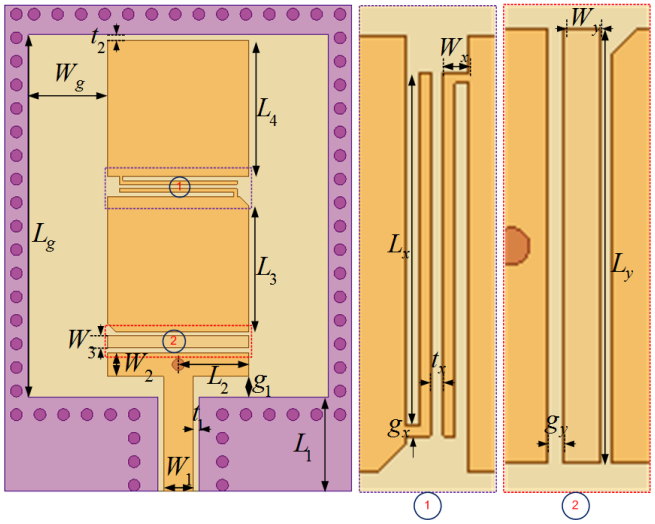

Fig. 2. Top and enlarged views of the proposed antenna.

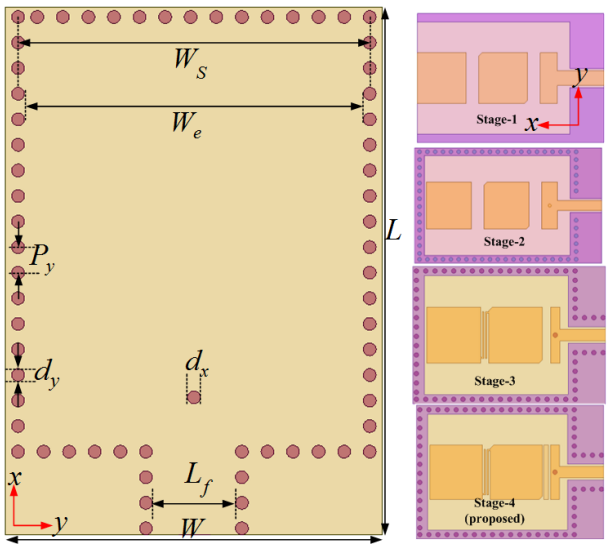

Fig. 3. Ground view and different design stages of the proposed antenna.

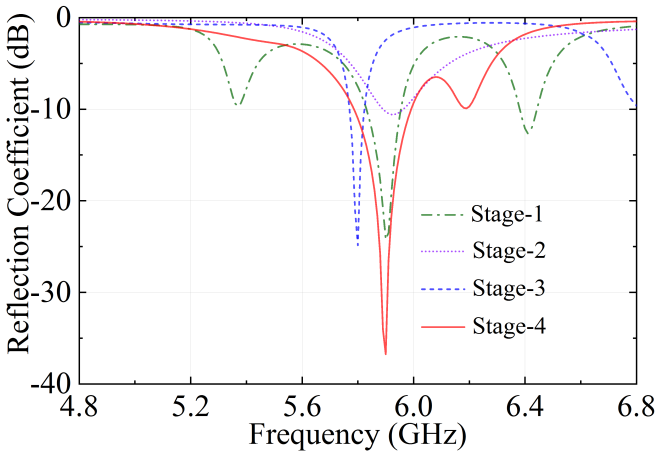

Fig. 4. Simulated reflection coefficient vs frequency plot at various stages.

[9]. Additionally, this antenna can find uses on vehicular platform, as shown in Fig. 1. The proposed antenna can enable different vehicle communications, including vehicle-to-pedestrian [10], vehicle-to-vehicle [11], vehicle-to-network [12] and vehicle-to-infrastructure [13] cases. The proposed antenna can have a wide application in future intelligent vehicles as the characteristics of this antenna fulfill the requirements for aerodynamic wireless devices used in modern vehicles for blind spot detection.

II. Design and Analysis of Proposed Antenna Structure

The geometry of the proposed antenna structure with the concept based on analysis of the resonance behavior is illustrated in Fig. 2. The top view of the proposed antenna is shown in Fig. 2 (left), and its enlarged feed and coupling sections are shown in Fig. 2 (right). Similarly, the bottom view and the various stages of the antenna design are illustrated in Fig. 3. The dielectric substrate used for the proposed antenna is Rogers $RO4232^{(TM)}$ 4232 (ϵ_r = 3.2, tan, δ = 0.0018, according to data sheet) of 1.524 mm thickness. All simulations were carried out using full-wave Ansys HFSS ver. 2020R2. The fabricated antenna sample was also verified experimentally..

The antenna is in the form of one planar side structure with a conductor-backed CPW (CB-CPW) feed. Two radiating patches and the gaps are cascaded in series. The first gap located between the patches includes two L-shape stubs, and the second, located between the patch and feed with two quarter-wave resonators, includes a narrow open stub ((see Fig. 2, top right)). These gaps play a crucial role in creating the electric coupling and are influencing the antenna resonant frequency. The feed section (Fig. 3, top right corner) includes a pair of quarter-wave resonators, which helps to get a better impedance match. A shorting pin located between the quarter-wave resonators is also used for matching improvement. In addition, the combination of shorting pin and two quarter-wave resonators falls in the category of proximity feed with the main objective to suppress the unwanted harmonics as reported in [14]–[16]. The dimensions of a narrow open stub are $W_3 \times 2L_2$. The L-shape stubs are defined by g_x, t_x, L_x and W_x. The gaps between the two patches are marked as (1) and (2) (see Fig. 2). We stress once more that these stubs are improving the impedance matching and radiation characteristics. The most important parameters are the gap t_x between these pair of stubs, and g_y ; they define electric coupling between patches. The truncated corner is used to achieve the strong surface current. The structure dimensions are $W_g = 5.95$, $L_g = 36.75$, $L_3 = 11.5$, $L_4 = 12$, $L_2 = 6.8$, $P_y = 2$, $d_y = 1$ $d_p = 1$, $g_1 = 1.75$, $t_2 = 0.5$, $t_1 = 0.4$,

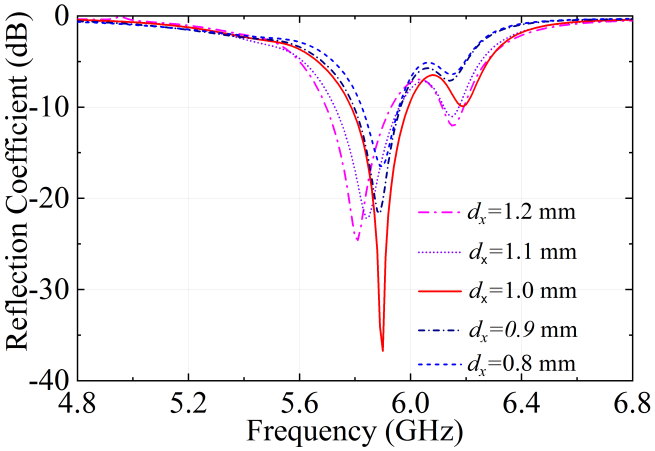

Fig. 5. Effect of shorting pin on reflection coefficient.

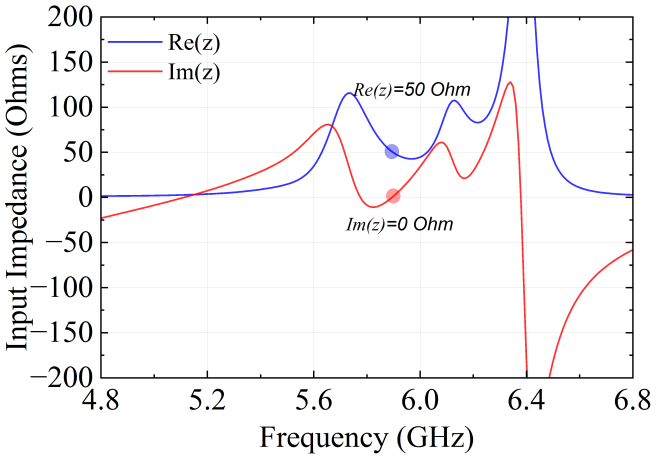

Fig. 6. Simulated input impedance vs frequency plot.

$L_1 = 8$, $W_2 = 2$, $W_1 = 2.5$, $W_3 = 1$, $L_x = 10$, $L_f = 7.5$, $g_x = 0.3$, $t_x = 0.4$, $w_x = 0.7$, $W_y = 1$, $g_y = 0.43$, $L_y = 2 \times L_2$, $L = 29.5$, $W = 41.25$, $W_e = 26.93$, $W_S = 27.5$, $h = 1.524$; unit: millimeters (see Fig. 1 and 2). The SIW parameters such as P_y, d_y, W_s, and $W_e$have been calculated following the methodic described in [17].

Four stage design process is used in the proposed antenna, as shown in Fig. 3 (see right side). The impact of each stages reflection coefficient is plotted in Fig. 4. In stage 4, the reflection coefficient is found to be better than at the other stages (stage 1, 2, and 3). To fix the diameter of shorting pin d_x, the parametric analysis is utilized in this work, as depicted in Fig. 5. When d_x is varied from 0.8 to 1.2 mm with a step size of 0.1 mm, the resonant frequencies are shifted from higher to the lower values. The reflection coefficient is the best at d_x=1 mm. In the end, the d_x is fixed at 1 mm. When the diameter d_x is 1 mm, then the real part of the input impedance at the desired frequency is around 50 Ω and, simultaneously, the imaginary part is approximately zero, as plotted in Fig. 6. The electric field distribution is plotted (both vector and magnitude) at 5.9 GHz, as shown in Fig. 7 (a). The surface current distribution is uniform, as shown in Fig. 7 (b), and hence, leads to an omnidirectional radiation pattern.

III. Validation and Discussions

The fabricated antenna prototype is tested experimentally using in a vector network analyzer (VNA) to measure the reflection coefficient, as shown in Fig. 8. The simulated and measured results are almost identical, as illustrated in Fig. 9. The measured resonant frequency (5.92 GHz) is slightly shifted (approximately 20 MHz) toward the higher values as compared to the simulated (5.9 GHz). The measured and simulated reflection coefficient is higher than 10 dB from 5.76 to 6.28 GHz and 5.74 to 6.0 GHz, respectively. The measured 10 dB reflection coefficient of fractional impedance bandwidth is 8.81%, whereas the simulated value is 4.24%.

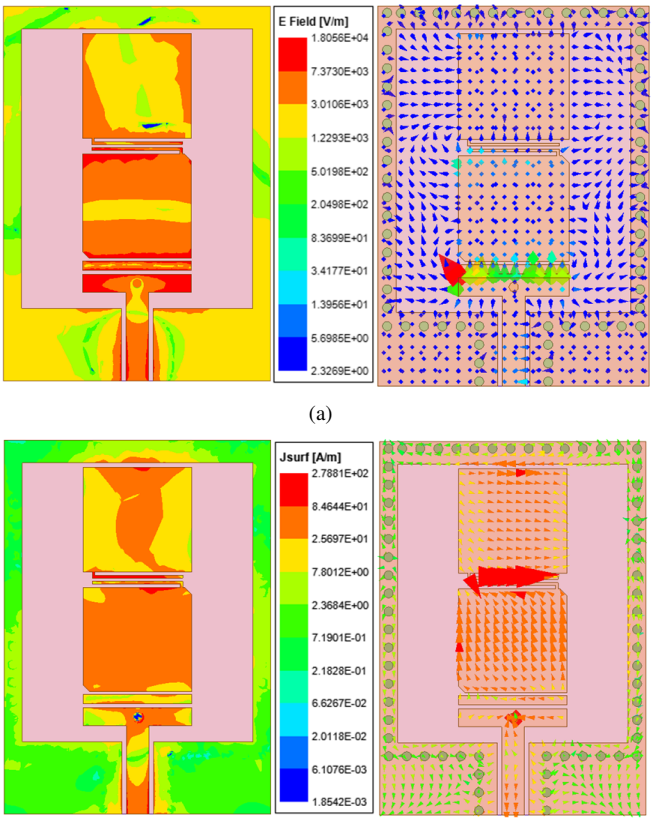

Fig. 7. Field distribution at 5.9 GHz: (a) Electric field and (b) Surface current.

It can be noticed that in the measured frequency shift and the measured fractional bandwidth the most important cause of difference between the simulated and measured results is the manual fill of metallic paste into the vias, and SMA connector and conductor losses.

The experimental and simulated values of the peak realized

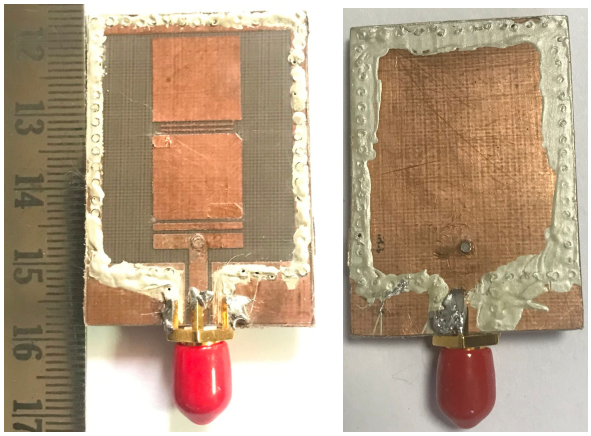

(a) (b)

Fig. 8. Fabricated prototype of proposed antenna: (a) Top view and (b) bottom view.

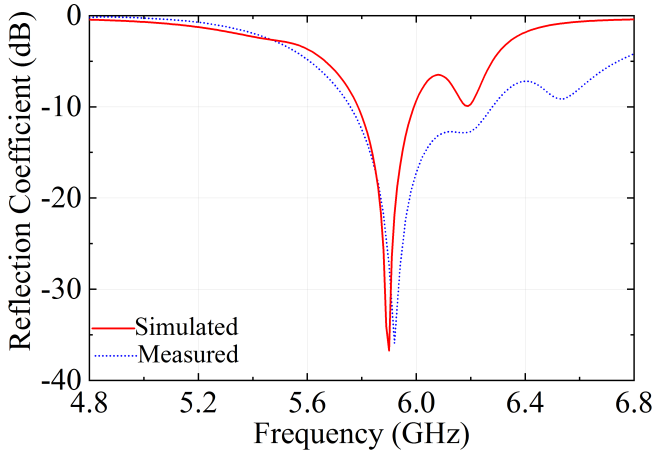

Fig. 9. Simulated and measured reflection coefficient.

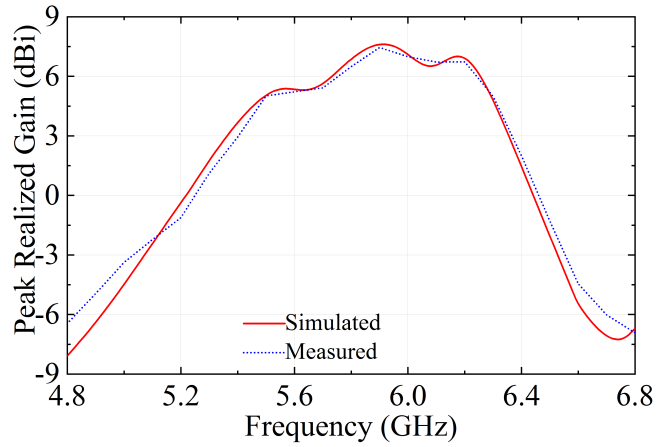

Fig. 10. Simulated and measured peak realized gain vs frequency.

gain are plotted in Fig. 10. The measured value of peak realized gain of 7.45 dBi (simulated: 7.62 dBi) is obtained at

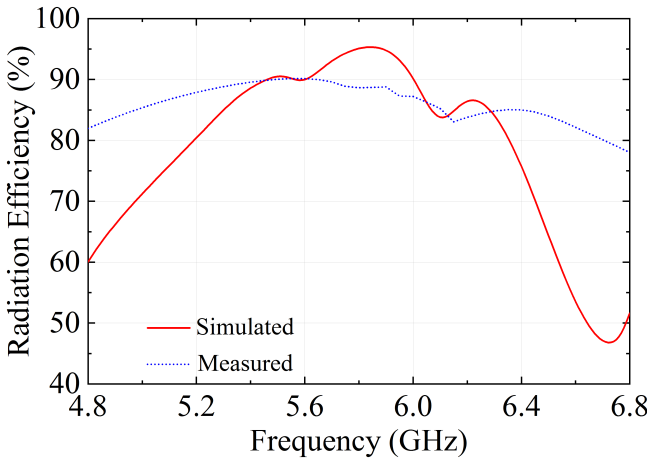

Fig. 11. Simulated and measured radiation efficiency vs frequency.

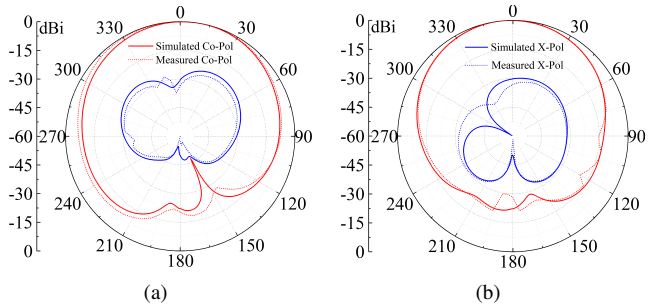

Fig. 12. Simulated and experimental normalized radiation pattern at 5.9 GHz: (a) E-plane, (b) H-plane.

resonant frequency. Similarly, the radiation efficiency is also measured using of Wheeler cap method [18], and the result is depicted in Fig. 11. The measured efficiency is 88.68% (simulated: 95%). The measured efficiency is lower than the simulation, which may be attributed to losses not considered in the experimental environment.

The measured normalized radiation patterns of E-plane and H-plane at 5.92 GHz are plotted, as shown in Fig. 12. The radiation pattern is omnidirectional on both planes. It can be observed that the simulated and experimental values of the front-to-back ratio is more than 25 dB. In contrast, the measured cross-polarization level in E-and H-planes are at -33 dB (simulated: -30 dB). The measured results are in good agreement with simulation results and the same has been verified all the above results.

IV. Conclusion

This paper describes the designed, fabricated, and measured the substrate integrated waveguide (SIW) cavity slot antenna for vehicles-to-vehicles communication applications operating in the DSRCS band (5.9 GHz). A commendable absolute impedance bandwidth of 520 MHz, with a peak-realized gain of 7.45 dBi, has been achieved. In addition,

the efficiency of 88.68%, and the cross-polarization below -33 dB have been achieved at 5.92 GHz in measurement. The experimental performance of the antenna ensures that it can be used as example, for aerodynamic wireless devices in intelligent vehicle for blind spot detection.

V. Acknowledgment

We would like to acknowledge Science and Engineering Research Board, Govt. of India, for providing the financial support to carry out this research under the Overseas Visiting Doctoral Fellowship Award No. SB/S9/Z-16/2016-V (2019 20). We also thank Mr. S. Gaur and Kamveer for their assistance in the fabrication and measurements carried out in this work. The financial assistance of NSERC, Canada (via grant RGPIN-2017-03719) is fully recognized

References

[1] D. Jiang and L. Delgrossi, "IEEE 802.11p: Towards an International Standard for Wireless Access in Vehicular Environments," in *VTC Spring 2008 - IEEE Vehicular Technology Conference*, 2008, pp. 2036–2040.

[2] S. Eichler, "Performance Evaluation of the IEEE 802.11p WAVE Communication Standard," in *2007 IEEE 66th Vehicular Technology Conference*, 2007, pp. 2199–2203.

[3] L. Liang, H. Peng, G. Y. Li, and X. Shen, "Vehicular Communications: A Physical Layer Perspective," *IEEE Transactions on Vehicular Technology*, vol. 66, no. 12, pp. 10 647–10 659, 2017.

[4] K. Abboud, H. A. Omar, and W. Zhuang, "Interworking of DSRC and Cellular Network Technologies for V2X Communications: A Survey," *IEEE Transactions on Vehicular Technology*, vol. 65, no. 12, pp. 9457–9470, 2016.

[5] X. Li, L. Ma, R. Shankaran, Y. Xu, and M. A. Orgun, "Joint Power Control and Resource Allocation Mode Selection for Safety-Related V2X Communication," *IEEE Transactions on Vehicular Technology*, vol. 68, no. 8, pp. 7970–7986, 2019.

[6] L. Yan, W. Hong, G. Hua, J. Chen, K. Wu, and T. J. Cui, "Simulation and Experiment on SIW Slot Array Antennas," *IEEE Microwave and Wireless Components Letters*, vol. 14, no. 9, pp. 446–448, 2004.

[7] G. Q. Luo, Z. F. Hu, L. X. Dong, and L. L. Sun, "Planar Slot Antenna Backed by Substrate Integrated Waveguide Cavity," *IEEE Antennas and Wireless Propagation Letters*, vol. 7, pp. 236–239, 2008.

[8] J. C. Bohorquez, H. A. Forero Pedraza, I. C. H. Pinzon, J. A. Castiblanco, N. Pena, and H. F. Guarnizo, "Planar Substrate Integrated Waveguide Cavity-Backed Antenna," *IEEE Antennas and Wireless Propagation Letters*, vol. 8, pp. 1139–1142, 2009.

[9] W. Wang, J. Wang, A. Liu, and Y. Tian, "A Novel Broadband and High-Isolation Dual-Polarized Microstrip Antenna Array Based on Quasi-Substrate Integrated Waveguide Technology," *IEEE Transactions on Antennas and Propagation*, vol. 66, no. 2, pp. 951–956, 2018.

[10] J. Zhu, Y. Yang, S. Li, S. Liao, and Q. Xue, "Dual-Band Dual Circularly Polarized Antenna Array Using FSS-Integrated Polarization Rotation AMC Ground for Vehicle Satellite Communications," *IEEE Transactions on Vehicular Technology*, vol. 68, no. 11, pp. 10 742–10 751, 2019.

[11] H. Xu, Z. Chen, H. Liu, L. Chang, T. Huang, S. Ye, L. Zhang, and C. Du, "Single-Fed Dual-Circularly Polarized Stacked Dielectric Resonator Antenna for K/Ka-Band UAV Satellite Communications," *IEEE Transactions on Vehicular Technology*, vol. 71, no. 4, pp. 4449–4453, 2022.

[12] Y. Q. Guo, Y. M. Pan, S. Y. Zheng, and K. Lu, "A Singly-Fed Dual-Band Microstrip Antenna for Microwave and Millimeter-Wave Applications in 5G Wireless Communication," *IEEE Transactions on Vehicular Technology*, vol. 70, no. 6, pp. 5419–5430, 2021.

[13] L. Liang, H. Peng, G. Y. Li, and X. Shen, "Vehicular Communications: A Physical Layer Perspective," *IEEE Transactions on Vehicular Technology*, vol. 66, no. 12, pp. 10 647–10 659, 2017.

[14] A. K. Nayak, R. Pachpole, and A. Patnaik, "A Dual-Band Antenna using IDC Based CRLH-TL Cell with Non-Uniform Finger Width," in *2019 IEEE Asia-Pacific Microwave Conference (APMC)*, 2019, pp. 798–800.

[15] A. K. Nayak and A. Patnaik, "Design and Testing of a Dual-band SIW Antenna Loaded with CRLH-TL Unit Cell," in *2019 IEEE Indian Conference on Antennas and Propogation (InCAP)*, 2019, pp. 1–4.

[16] ——, "SIW-Based Patch Antenna with Improved Performance," in *2017 IEEE Applied Electromagnetics Conference (AEMC)*, 2017, pp. 1–2.

[17] J.-D. Zhang, L. Zhu, Q.-S. Wu, N.-W. Liu, and W. Wu, "A compact microstrip-fed patch antenna with enhanced bandwidth and harmonic suppression," *IEEE Transactions on Antennas and Propagation*, vol. 64, no. 12, pp. 5030–5037, 2016.

[18] A. K. Nayak, R. Pachpole, and A. Patnaik, "Compact Symmetric Quarter Mode Substrate Integrated Waveguide (QMSIW) Antenna," in *2018 IEEE Indian Conference on Antennas and Propogation (InCAP)*, 2018, pp. 1–4.